Published in Applied Optics 31, issue 26, 5716-5723, 1992
which should be used for any reference to this work

Fan-out elements recorded as volume holograms: optimized recording conditions

H. P. Herzig, P. Ehbets, D. Prongué, and R. Dändliker

The recording of efficient fan-out elements as volume holograms is investigated by using the coupled-wave theory. In contrast to the results published in the standard literature, we find that the efficiency and the uniformity of regular fan-out elements depend strongly on the relative phases of the object waves, at least, if the thickness of the hologram is less than ~50 wavelengths. High efficiency and uniformity can be achieved by optimized recording conditions. At the same time, the required dynamic range of the holographic material becomes minimum.
Key words: Fan-out element, coupled-wave theory, volume hologram.

I. Introduction

Optical fan-out elements divide a single laser beam into a regular array of equally intense light spots in one or two dimensions. They are used in many applications of modern optics, such as parallel optical processing and fiber-optic communication. Currently fan-out elements are fabricated synthetically as surface-relief phase structures by using microfabrication techniques (e.g., see Ref. 1, Sec. 6). Such elements are Dammann gratings,[2] multilevel gratings,[3] or continuous surface-relief structures.[4] However, proper modulation at large carrier frequencies (>1000 lines/mm) is difficult to achieve by mask projection. Therefore interferometrically recorded holograms are still of interest for realizing off-axis elements and large fan-out numbers. This paper deals with the recording of efficient fan-out elements in thick volume holograms. We have applied the coupled-wave theory for studying recording conditions for high diffraction efficiency and uniformity of the generated beam array.

Papers on the coupled-wave theory for multiple beam recording predict high efficiency for replaying N waves, and only a weak dependence of interactions between the beams because of the highly selective Bragg condition.[5] This would suggest that the recording of fan-out elements is an easy task. However, experimental results show the difficulties in recording uniform fan-out elements as volume holograms and the precautions that are necessary for generating a uniform distribution of the irradiance in the hologram plane.[6] Fundamental difficulties are explained in terms of recording nonlinearity. By using the coupled-wave theory, we have found that even in the case of prefect linearity a hologram does not generate a uniform fan-out.[7] We demonstrate how to apply the coupled-wave theory to the special problem of regular fan-out elements. These elements are called degenerated because all gratings with equal periodicity diffract light in the same direction and must be added coherently. As a consequence, the results for efficiency and uniformity depend strongly on the relative phases of the recorded object waves.

The authors are with the Institute of Microtechnology, University of Neuchâtel, Rue A.-L. Breguet 2, Neuchâtel CH-2000, Switzerland.

II. Simultaneous Recording with Minimum Intermodulations

A fan-out element can be fabricated by recording a hologram of N object waves $E_i(\mathbf{x}) = A_i \exp(-j\mathbf{k}_i\mathbf{x} + j\phi_i)$ with a reference wave $E_0(\mathbf{x}) = A_0 \exp(-j\mathbf{k}_0\mathbf{x} + j\phi_0)$. The basic configuration is shown in Fig. 1. The waves are characterized by wave vectors $\mathbf{k}_i = (k_i^y, k_i^z)$, amplitudes A_i, and phases ϕ_i, where $\mathbf{x} = (y, z)$ are the coordinates. Only the s polarization is considered.

We assume that the recording material responds linearly to the accumulated energy during exposure, i.e.,

$$\epsilon(y, z) = \epsilon_a + \delta \left| \sum_{i=1}^{N} E_i + E_0 \right|^2. \qquad (1)$$

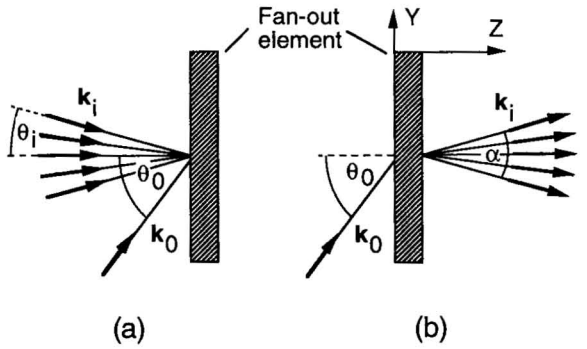

Fig. 1. (a) Recording and (b) readout of fan-out elements. The angles are defined inside the recording medium with refractive index $n = \sqrt{\epsilon_a}$ [see Eq. (1)]; α is the full fan-out angle.

The dielectric permittivity $\epsilon(y, z)$ after exposure then becomes

$$\epsilon(y, z) = \epsilon_a' + \sum_{i=1}^{N} \Delta\epsilon_{0i} \cos(\mathbf{K}_{0i}\mathbf{x} - \Phi_{0i}) + \sum_{q>p=1}^{N} \Delta\epsilon_{pq} \cos(\mathbf{K}_{pq}\mathbf{x} - \Phi_{pq}), \quad (2)$$

where $\Phi_{pq} = \phi_p - \phi_q$ and $\Delta\epsilon_{pq} = 2\delta A_p A_q$. Besides the desired N primary gratings $\mathbf{K}_{0i} = \mathbf{k}_0 - \mathbf{k}_i$, $N(N-1)/2$ unwanted intermodulation gratings $\mathbf{K}_{pq} = \mathbf{k}_p - \mathbf{k}_q$ are recorded. At readout, they generate intermodulation waves, which are coupled with the desired reconstruction beams. As a consequence, efficiency and uniformity of the fan-out suffer.

One possibility of reducing the intermodulations with respect to the primary gratings is to increase the reference-to-object beam ratio B (see Ref. 5), which is defined by

$$B = \frac{A_0^2}{\sum_{i=1}^{N} A_i^2}. \quad (3)$$

Then the modulations of the desired primary gratings become dominant ($\Delta\epsilon_{0i} \gg \Delta\epsilon_{pq}$). Unfortunately this method requires a high dynamic range of the recording material.

It was shown in an earlier paper that for on-axis regular fan-out elements the intermodulation gratings can be nearly perfectly eliminated.[4] In the case of regular elements, the projections $K_{pq}^{\,y}$ of the grating vector $\mathbf{K}_{pq}$ in the hologram plane (y axis) are all integer multiples of the lowest frequency $2\pi\nu$, which is formed by the interference between two neighboring object beams. Thus we can write the intermodulation term in Eq. (2) as

$$\sum_{q>p}^{N} \Delta\epsilon_{pq} \cos(\mathbf{K}_{pq}\mathbf{x} - \Phi_{pq}) = \sum_{q>p}^{N} \Delta\epsilon_{pq} \cos(2\pi m\nu y + K_{pq}^{\,z} z - \Phi_{pq}), \quad (4)$$

where $m = p - q$. There are $N - 1$ gratings with $m = 1$, $N - 2$ gratings with $m = 2$, etc. By adding the gratings with the same frequency but with optimized phase shifts Φ_{pq}, one can minimize the intermodulations.[4] Note that the grating with the highest frequency ($m = N - 1$) cannot be canceled because it appears only once.

The intermodulations vary in the z direction with $K_{pq}^{\,z}$ [Eq. (4)]. Consequently, they can be minimized for only one specific plane parallel to the hologram plane (z = constant). For on-axis object beams, as shown in Fig. 1, the z variation is rather slow, i.e., $K_{pq}^{\,z}$ is small. The largest component $K_{pq}^{\,z}$ is formed by the interference between the central beam propagating in the direction of the z-axis and the marginal beams of the fan-out. We obtain

$$(K_{pq}^{\,z})_{\max} = \frac{2\pi}{\lambda} n \left(1 - \cos\frac{\alpha}{2}\right) = \frac{2\pi}{\Lambda}, \quad (5)$$

where λ is the wavelength, α is the full angle ($\mathbf{k}_1$, $\mathbf{k}_N$) of the fan-out, n is the refractive index, and Λ is the periodicity of the grating $(K_{pq}^{\,z})_{\max}$. The intermodulations remain small within a depth h of $\pm\Lambda/10$, i.e.,

$$h = \frac{\Lambda}{5} = \frac{\lambda}{5n[1 - \cos(\alpha/2)]}. \quad (6)$$

We can conclude that for the geometry shown in Fig. 1 the hologram plane must be normal to the z axis within the tolerances given by Eq. (6). This restricts the optimum recording geometry.

For thick holograms the off-Bragg interactions become negligible, and, therefore, the phases of the object waves are irrelevant. In this case the recording geometry is not restricted by Eq. (6).

III. Coupled-Wave Equations

Below we derive the coupled-wave equations for regular fan-out elements. The electrical field has to fulfill the Helmholtz equation

$$\Delta E(y, z) + k^2\epsilon(y, z)E(y, z) = 0, \quad (7)$$

where $k = (2\pi/\lambda)$, and $\epsilon(y, z)$ as determined by Eq. (2).

The total electric field inside the hologram is written as a sum of M plane waves diffracted in different directions:

$$E(y, z) = E_0(y, z) + \sum_{i=1}^{N} E_i(y, z) + \sum_{i=N+1}^{M} E_i(y, z), \quad (8)$$

where the first N waves are the desired object waves. Each component of the electric field is of the form

$$E_i(y, z) = B_i(z)\exp(-j\mathbf{k}_i\mathbf{x}), \quad (9)$$

where $B_i(z)$ are complex amplitudes.

The waves $E_i(y, z)$ are generated by diffraction of an incident beam ($\mathbf{k}_m$) at a grating $\mathbf{K}_{pq}$. The wave vectors $\mathbf{k}_i$ are then determined by the beta-value construction, namely

$$k_i^{\,y} = k_m^{\,y} - K_{pq}^{\,y}, \qquad q > p = 0, \ldots, N-1; \quad i, m = 0, \ldots, M. \quad (10)$$

For the z components we obtain

$$k_i^z = [k^2\epsilon_a - (k_i^y)^2]^{1/2}. \quad (11)$$

The coupled-wave equations are now obtained by introducing the electric field [Eq. (8)] into the Helmholtz equation (7). This yields

$$\frac{dC_m}{dz}\cos\theta_m = -j\sum_{n=0}^{M}\mathscr{W}_{mn}C_n, \qquad m = 0, \ldots, M, \quad (12)$$

where $C_i = B_i \exp(-jk_i^z)$. The reason for this substitution is to separate the wave parameters, which are described by the coefficients C_i, and the independent grating parameters, which are described by the matrix $\mathscr{W}_{mn}$. Note that the matrix must be Hermitian, i.e., $\mathscr{W}_{mn} = \mathscr{W}_{nm}^*$, and that the diagonal elements are equal to zero, i.e., $\mathscr{W}_{mm} = 0$.

For a simple coupling between two waves E_m and E_n through one grating $\mathbf{K}_{pq}$, we get

$$\mathscr{W}_{mn} = \chi_{pq} = \kappa_{pq}\exp[j(-K_{pq}^z + \Phi_{pq})]. \quad (13)$$

$\kappa_{pq} = k\Delta\epsilon_{pq}/4$ is Kogelnik's coupling coefficient for the grating $\mathbf{K}_{pq}$.

We have to consider that each beam E_m diffracts at all gratings. In our degenerated case all gratings with equal periodicity, i.e., equal K_{pq}^y, diffract light in the same direction. Their coupling coefficients have to be added coherently, which means that

$$\mathscr{W}_{mn} = \sum \chi_{pq}, \quad (14)$$

for $q - p =$ constant.

Figure 2 shows the spectrum of the waves included in our model for a fan-out of $N = 3$ and possible interactions for object wave (O wave) number 2 through the three primary gratings $\mathbf{K}_{01}$, $\mathbf{K}_{02}$, and $\mathbf{K}_{03}$, and the three intermodulation gratings $\mathbf{K}_{12}$, $\mathbf{K}_{23}$, and $\mathbf{K}_{13}$. For further reading, I waves are the intermodulation waves generated by diffraction of the readout wave at the intermodulation gratings $\mathbf{K}_{pq}$, and S waves are the secondary waves generated by diffraction of the object waves at the intermodulation gratings $\mathbf{K}_{pq}$.

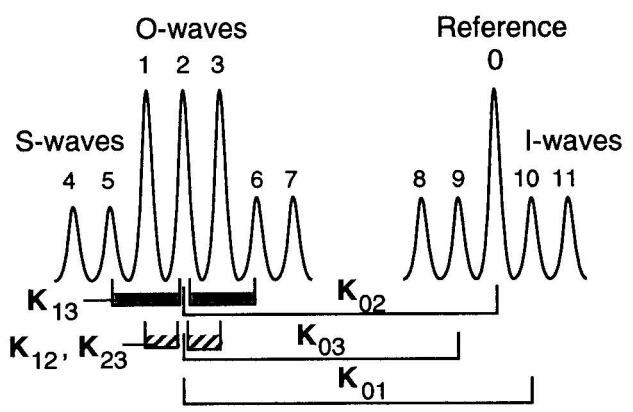

Fig. 2. Spectrum of the waves included in our model for a fan-out of $N = 3$, and possible interactions for object wave (O wave) no. 2 through primary gratings $\mathbf{K}_{0i}$ and intermodulation gratings $\mathbf{K}_{pq}$.

For a fan-out of N waves, we have made the following assumptions for our coupled-wave model:

- Simultaneous recording of N object waves and one reference wave leads to N primary gratings $\mathbf{K}_{0i}$ and $N(N-1)/2$ intermodulation gratings $\mathbf{K}_{pq}$, where $q > p = 1, \ldots, (N-1)$.
- The primary gratings are thick; only one diffraction order is considered.
- The intermodulation gratings are considered to be optically thin; the $\pm$ first diffraction orders are included.
- At readout, N object waves (O waves), $2(N-1)$ secondary waves (S waves), and $2(N-1)$ intermodulation waves (I waves) are generated.
- Any possible coupling between the waves E_m through the gratings $\mathbf{K}_{0i}$ and $\mathbf{K}_{pq}$ are accepted.
- Coupling coefficients χ_{pq} of gratings with equal periodicity, i.e., equal K_{pq}^y, are added coherently.

IV. Numerical Results

The coupled-wave equations (12) have been solved by numerical integration with a Runge–Kutta equation. The boundary conditions for transmission holograms at $z = 0$ are $C_0 = 1$ and $C_i = 0$ for $i = 1, \ldots, M$.

The diffraction efficiency η_T of all object waves is obtained from Eq. (15):

$$\eta_T = \sum_{i=1}^{N}\eta_i,$$

with

$$\eta_i = \frac{\cos\theta_i}{\cos\theta_0}|C_i|^2, \qquad i = 1, \ldots, N. \quad (15)$$

The uniformity error e, which is important for fan-out elements, is described by

$$e = \frac{\eta_{i_{max}} - \eta_{j_{min}}}{\langle\eta_i\rangle}. \quad (16)$$

Below we distinguish between the corrected case and the uncorrected case. The corrected case has optimized phases Φ_{pq} for minimum intermodulations at the point z = 0, i.e., at the surface of the holographic emulsion. Except in the trivial case of three waves, the phases Φ_{pq} have been determined by numerical optimization.[4] In the uncorrected, worst case, a constant phase is assumed. We have calculated the results for a fan-out of $N = 3$ (Fig. 3 and Table I) and $N = 9$ (Fig. 4 and Table II). The following values have been used for the calculations:

- For three object beams: $\phi_1 = \phi_3 = 0$, $\phi_2 = \pi/2$.
- For nine object beams: $\phi_1 = \phi_9 = 1.77219$, $\phi_2 = \phi_8 = 0.13512$, $\phi_3 = \phi_7 = 3.88710$, $\phi_4 = \phi_6 = 2.45465$, $\phi_5 = 3.14159$ rad.
- Uncorrected worst case: $\phi_i = 0$.

Note that $\Phi_{pq} = \phi_p - \phi_q$.

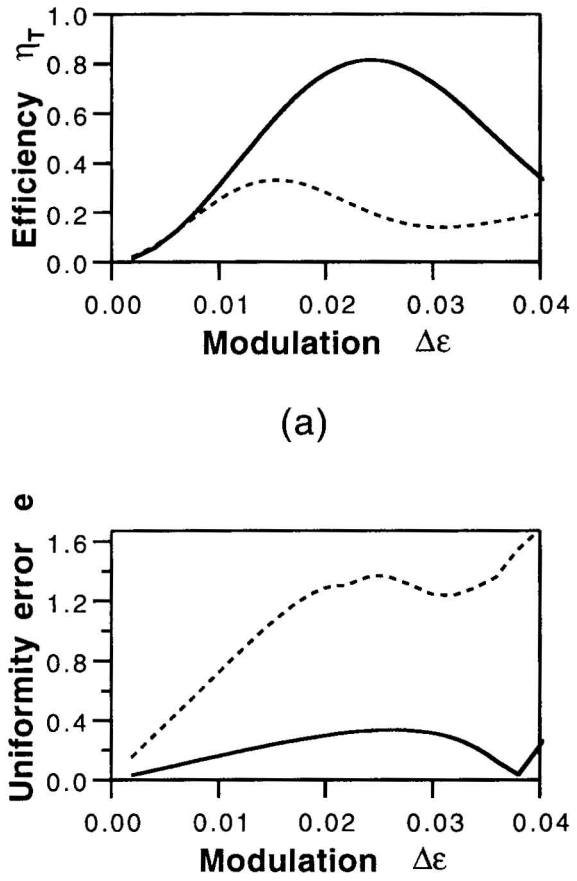

Fig. 3. Results for a fan-out of $N = 3$: (a) Total useful diffraction efficiency η_T versus the modulation amplitude $\Delta\epsilon$. The solid curve corresponds to the case of corrected phases and the dashed curve corresponds to the worst case; (b) uniformity error e versus $\Delta\epsilon$. The recording parameters are $\lambda = 0.488$ μm, $n = 1.5$, $B = 1$, $\theta_0 = 30°$, $\Delta\alpha = 1°$, and $d = 15$ μm.

Table I. Results for a Fan-out of $N = 3$[a]

Interbeam Angle, $\Delta\alpha$	Beam Ratio, B	Modulation, $\Delta\epsilon$	Maximum Useful Diffraction Efficiency, η_T	Uniformity Error, e	
0.1°	1	0.013	0.23	0.63	uncorrected
	5	0.017	0.40	0.15	
	10	0.018	0.44	0.12	
0.1°	1	0.021	0.62	0.20	corrected
	5	0.022	0.78	0.28	
	10	0.024	0.81	0.30	
0.1°	1	0.021	0.62	0.20	corrected[b]
1°	1	0.016	0.32	1.10	uncorrected
	5	0.020	0.55	0.58	
	10	0.021	0.60	0.41	
1°	1	0.024	0.82	0.33	corrected
	5	0.026	0.94	0.16	
	10	0.026	0.95	0.12	
1°	1	0.024	0.82	0.32	corrected[b]
5°	1	0.024	0.75	1.73	uncorrected
	5	0.026	0.94	0.75	
	10	0.026	0.97	0.51	
5°	1	0.025	0.85	1.35	corrected
	5	0.026	0.96	0.80	
	10	0.026	0.97	0.60	
5°	1	0.025	0.96	0.60	corrected[b]

[a]The recording parameters are $\lambda = 0.488$ μm, $n = 1.5$, $\theta_0 = 30°$, and $d = 15$ μm.
[b]See Section V.

Figures 3 and 4 show the total useful diffraction efficiency η_T and the uniformity error e as a function of the modulation amplitude $\Delta\epsilon = \Delta\epsilon_{0i}$ of one primary grating for $N = 3$ and $N = 9$, respectively. The corrected cases (solid curve) show a high diffraction efficiency and a good uniformity. The efficiency increases up to a maximum with increasing modulation, similar to the behavior of a single grating in a volume hologram. In the uncorrected cases (dashed curve), the efficiency is low and the uniformity is poor. Note that the modulation amplitude $\Delta\epsilon$ that is necessary for optimum efficiency is approximately $\sqrt{N}$ smaller than in the case of a single grating.

The angular separation of the fan-out is indicated by the angle $\Delta\alpha = \theta_{i+1} - \theta_i$ between two neighboring object beams. Tables I and II present the maximum diffraction efficiency η_T for different interbeam angles $\Delta\alpha$ and different beam ratios B, again for $N = 3$ and $N = 9$, respectively. From the numerical results we can clearly see the importance of using corrected phases for the object beams. For a reference-to-object beam ratio equal to unity, the fan-out element already possesses good characteristics. For example, for $N = 9$ and $\Delta\alpha = 0.1°$ the maximum diffraction efficiency becomes $\eta_{T_{max}} \sim 94\%$ with a relatively good uniformity of $e < 0.2$.

All calculations have been made with the following parameters: wavelength $\lambda = 0.488$ μm, refractive index of the holographic medium $n = 1.5$, thickness of the medium $d = 15$ μm, and reference beam angle $\theta_0 = 30°$.

V. Discussion

Here we try to explain the results obtained by our coupled-wave model. We have found that for small interbeam angles $\Delta\alpha$ the corrected phases give a much better efficiency. For larger angles the effect is less significant. A similar behavior is observed for the uniformity error e, except that for large $\Delta\alpha$ the uniformity may become bad.

In the ideal case, the Bragg condition is fulfilled for only the reconstruction of the desired N object waves through the primary gratings $\mathbf{K}_{0i}$. In reality, an unwanted cross coupling between the object waves (O waves) and intermodulation waves (I waves) through the efficient gratings $\mathbf{K}_{0i}$ also occur, as shown in Fig. 2. These interactions are influenced by the phases Φ_{0i}, but not by the beam ratio B (see results for $\Delta\alpha = 0.1°$). For fan-out elements, neighboring beams are rather close; thus the interactions are still close to the Bragg condition. Figure 5 shows the typical off-Bragg behavior of a thick volume grating. We

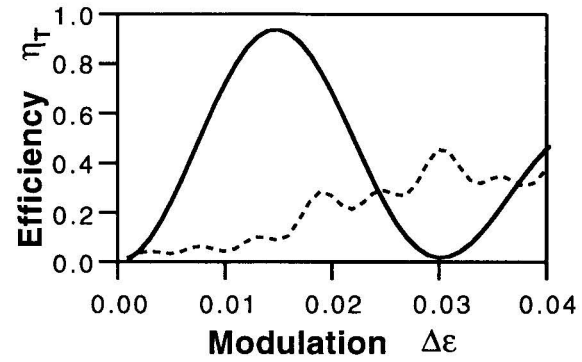

(a)

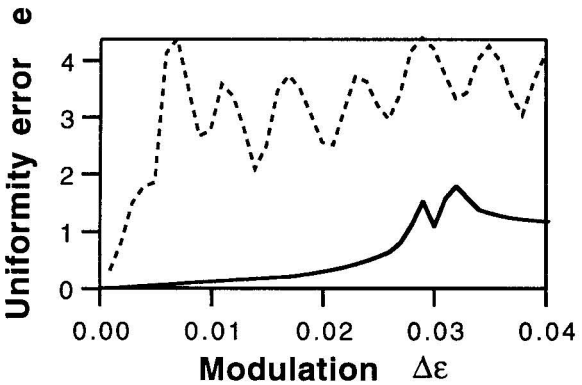

(b)

Fig. 4. Results for a fan-out of $N = 9$: (a) Total useful diffraction efficiency η_T versus the modulation amplitude $\Delta\epsilon$. The solid curve corresponds to the case of corrected phases and the dashed curve corresponds to the worst case; (b) uniformity error e versus $\Delta\epsilon$. The recording parameters are $\lambda = 0.488$ μm, $n = 1.5$, $B = 1$, $\theta_0 = 30°$, $\Delta\alpha = 0.1°$, and $d = 15$ μm.

assume that wave i fulfills the Bragg condition. It has been generated by diffraction at the grating $\mathbf{K}_{0i}$. The neighboring wave $i + 1$ can also receive light through the same grating $\mathbf{K}_{0i}$, but this interaction is now off-Bragg. The coupling remains efficient if the phase mismatch is less than 2π. We have applied this criterion to the arrangement shown in Fig. 1. It turns out that these off-Bragg interactions are important for a hologram thickness that is smaller than

$$t = \lambda/(n \tan \theta_0 \Delta\alpha), \tag{17}$$

where $\Delta\alpha = \alpha/(N - 1)$ is the interbeam angle between two neighboring beams, θ_0 is the reference beam angle, λ is the wavelength, and n is the refractive index. Consequently for a larger interbeam angle $\Delta\alpha$ and thicker holograms the fan-out properties become less sensitive to the phases. This can be observed for the efficiencies but not for the uniformities.

Table II. Results for a Fan-out of $N = 9$[a]

Interbeam Angle, $\Delta\alpha$	Beam Ratio, B	Modulation, $\Delta\epsilon$	Maximum Useful Diffraction Efficiency, η_T	Uniformity Error, e	
0.1°	1	0.030	0.45	4.20	uncorrected
	5	0.050	0.34	4.10	
	10	0.038	0.47	3.91	
0.1°	1	0.015	0.94	0.19	corrected
	5	0.015	0.97	0.12	
	10	0.015	0.98	0.12	
0.1°	1	0.015	0.94	0.19	corrected[b]
1°	1	0.021	0.30	3.21	uncorrected
	5	0.036	0.41	2.93	
	10	0.042	0.42	4.70	
1°	1	0.015	0.96	1.51	corrected
	5	0.015	0.97	0.73	
	10	0.015	0.98	0.57	
1°	1	0.015	0.98	0.35	corrected[b]
3°	1	0.024	0.77	1.09	uncorrected
	5	0.016	0.89	0.86	
	10	0.016	0.94	0.79	
3°	1	0.016	0.83	3.95	corrected
	5	0.015	0.95	1.68	
	10	0.015	0.97	1.11	
3°	1	0.016	0.83	2.44	corrected[b]

[a]The recording parameters are $\lambda = 0.488$ μm, $n = 1.5$, $\theta_0 = 30°$, and $d = 15$ μm.
[b]See Section V.

We have assumed that, at recording, the N amplitudes of the object beams are equal $A_i = 1$. For small interbeam angles $\Delta\alpha$, a perfect uniformity ($e < 0.01$) is achieved by adjusting the amplitudes A_i.

There are different reasons for uniformity errors. One reason is that the coupling coefficients depend on the directions of the wave propagation. Another reason is that, for optimized phases, the intermodulation gratings $\mathbf{K}_{pq}$ are canceled only within a depth h, which is given by Eq. (6). For larger fan-out angles α, the depth h becomes short, and therefore undesired intermodulation gratings are recorded. As a result the uniformity error increases, as observed for $\Delta\alpha = 5°$, i.e., $\alpha = 10°$ (Table I), and $\Delta\alpha = 3°$, i.e., $\alpha = 24°$

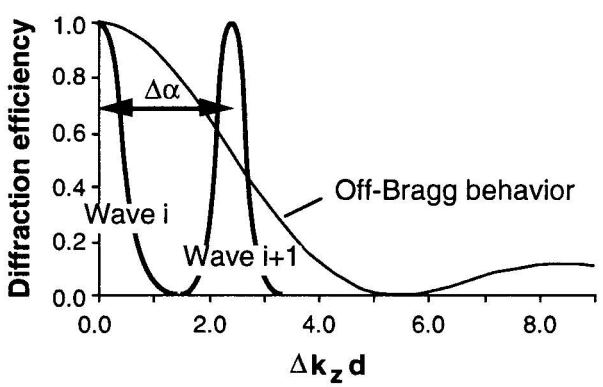

Fig. 5. Wave i fulfills the Bragg condition when diffracted at the grating $\mathbf{K}_{0i}$, whereas wave $\mathbf{K}_{i+1}$ is off-Bragg. If the phase mismatch becomes 2π, the coupling is no longer efficient.

(Table II). This error can be reduced by the beam ratio B or by the position of the plane of minimum intermodulations. As already mentioned above, the corrected case has optimized phases Φ_{pq} for minimum intermodulations at the point z = 0, i.e., at the surface of the holographic emulsion. If we would place the plane with minimum intermodulation in the center of the hologram at $z = d/2$, the uniformity error decreases significantly (see footnotes *b* in Tables I and II).

The uniformity problems observed for large angles between the beams are created by the thin intermodulation gratings $\mathbf{K}_{pq}$. We think that these gratings are not sufficiently described in our model by taking into account the ±1st orders only. A more rigorous theory is necessary to treat them exactly for large angles also.

Note that for sequentially recorded holograms the intermodulation gratings $\mathbf{K}_{pq}$ are not recorded, whereas the strong cross coupling through primary gratings $\mathbf{K}_{0i}$ is present.

VI. Dynamic Range

A holographic emulsion has a limited dynamic range that depends on the material and the thickness. For an optimum hologram recording the exposure energy must be within the dynamic range. If the exposure is increased about saturation, the emulsion does not generate a higher index modulation. For a high reference-to-object beam ratio and large fan-outs the limited dynamic range becomes important. We show that recording with optimized phases requires a lower dynamic range.

During recording, N object waves $E_i(\mathbf{x}) = A \times \exp[-j(\mathbf{k}_i\mathbf{x} + \phi_i)]$ and one reference wave $E_0(\mathbf{x}) = A_0 \exp[-j(\mathbf{k}_0\mathbf{x} + \phi_0)]$ are present. As shown in Eq. (1), the irradiance $I(\mathbf{x})$ in the hologram plane is given by

$$I(\mathbf{x}) = \left|\sum_{i=1}^{N} E_i + E_0\right|^2$$

$$= A_0^2 + NA^2 + 2A_0A\sum_{i=1}^{N}\cos(\mathbf{K}_{0i}\mathbf{x} - \Phi_{0i})$$

$$+ 2A^2\sum_{q>p=1}^{N}\cos(\mathbf{K}_{pq}\mathbf{x} - \Phi_{pq}), \qquad (18)$$

with $\Phi_{pq} = \Phi_p - \Phi_q$ and $\mathbf{K}_{pq} = \mathbf{k}_p - \mathbf{k}_q$.

Figure 6 shows the irradiance $I(\mathbf{x})$ in the hologram plane (y axis) for optimized phases and for the worst case ($\Phi_{0i} = \Phi_{pq} = 0$), respectively. Both cases are calculated for maximum contrast, i.e., $I_{\min} = 0$ and for the same maximum irradiance $I_{\max}$. In the uncorrect case ($\Phi_{0i} = \Phi_{pq} = 0$) all gratings are in phase at $x = 0$ and $y = 0$; thus all amplitudes add up and produce a high maximum intensity. In the corrected case with the optimized phases, however, the primary gratings $\mathbf{K}_{0i}$ are never all in phase at the same position, and the intermodulation term, which contains the gratings $\mathbf{K}_{pq}$, disappears nearly perfectly.

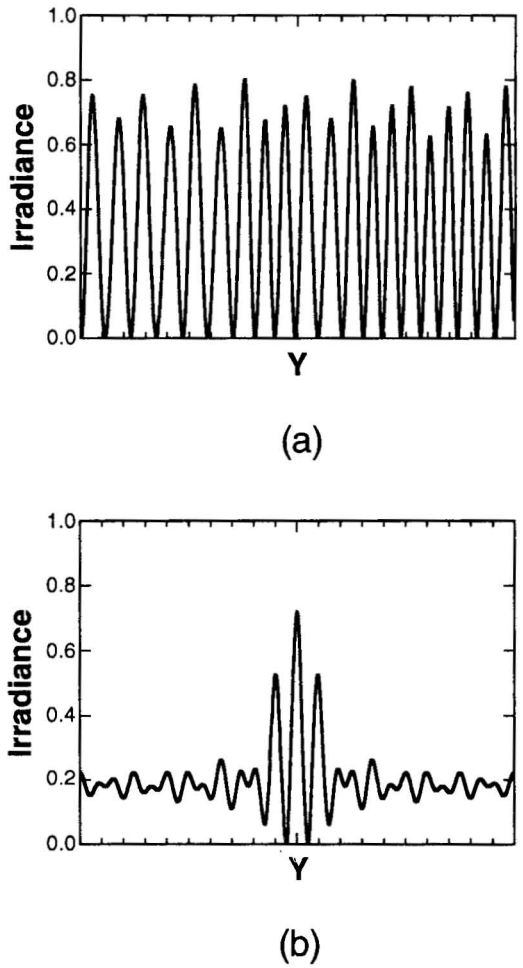

Fig. 6. Interference pattern in the hologram plane (y axis) of nine object beams with a reference wave for (a) optimized phases, (b) worst case, for the same maximum modulation level.

Then the first summation in Eq. (18) yields $2A_0A\sqrt{N}$ and the second summation, i.e., the intermodulations, can be omitted. The maximum and minimum values of the irradiance are found to be

$$I_{\max} = (A_0 + \sqrt{N}A)^2, \qquad I_{\min} = (A_0 - \sqrt{N}A)^2, \qquad (19)$$

for the corrected case, and

$$I_{\max} = (A_0 + NA)^2, \qquad I_{\min} = (A_0 - NA)^2, \qquad (20)$$

for the uncorrected case, where N is the number of fan-out beams and A is the amplitude of the object waves for the recording. Maximum contrast is obtained for $I_{\min} = 0$, which gives the relations $A_0 = \sqrt{N}A$ and $A_0 = NA$ for the two cases, respectively. Then we get a reference-to-object ratio of $B = 1$ for the optimized phases from Eq. (3), whereas $B = N$ for the uncorrected case, which means that the corrected case requires considerably less reference irradiance.

The modulation of the dielectric permittivity $\Delta\epsilon_{0i}$ for the primary gratings $\mathbf{K}_{0i}$, as shown in Eq. (2), is proportional to $2A_0A$. Assuming that the recording

material saturates at a level corresponding to an irradiance of $I_{max} = I_s$, we then find from Eqs. (19) and (20), with $I_{min} = 0$, that

$$\Delta\epsilon_{0i} \propto 2A_0A = 2\sqrt{N}A^2 = I_s/2\sqrt{N} \qquad (21)$$

for the corrected case, and

$$\Delta\epsilon_{0i} \propto 2A_0A = 2NA^2 = I_s/2N \qquad (22)$$

for the uncorrected case, which means that the recorded modulation $\Delta\epsilon_{0i}$ for the primary gratings is $\sqrt{N}$ times higher for the optimized phases. Besides the fact that the fan-out is more efficient in the case of corrected phases, as shown in Figs. 3 and 4, the required modulation amplitude $\Delta\epsilon$ for maximum efficiency can be obtained more easily within the limited dynamic range of the recording material.

VII. Recording Optimized Fan-Out Elements

Figure 7(a) shows the recording setup for on-axis fan-out holograms. The object is an array of coherent sources. The optimized phases ϕ_i can be obtained by different techniques. One possibility is to illuminate a pinhole array, followed by an appropriate phase plate. Another is to use computer-generated holograms or kinoforms to generate the desired array (see Figs. 6 and 7 in Ref. 4). If the sources are in the front focal plane of the lens ($d = f$), the recorded element is nonfocusing; for greater object distances ($d > f$) it becomes focusing. Figure 7(b) shows the off-axis equivalent. Because of the limited depth of the optimum plane [Eq. (6)], the source array and the holographic optical element must be parallel.

If the lens is removed, we get a focusing fan-out element. However, the optimized phases generate a uniform illumination only if the hologram is in the far field, i.e., at a distance $d > (Ns)^2/\lambda$ [see Fig. 8(a)]. Another method of fabricating focusing fan-out elements without a lens uses the self-imaging properties of large periodic structures.[8] In this case the object is a regular array of coherent sources with identical phases $\phi_i = 0$. Considering the beam propagation in free space, we find planes of reduced intermodulations that are suitable for recording efficient holograms. These planes are parallel to the object plane, as in the case of optimized phases. In Fig. 8(b) we incline the object; thus we must also incline the hologram. The self-imaging (Talbot) distance is proportional to s^2 and for inclined objects is proportional to $(s \cos\theta)^2$. If we incline a regularly spaced two-dimensional array (same spacing s in the x and the y directions) with respect to the y axis, we get two different distances for the optimum planes, depending on s^2 and $(s \cos\theta)^2$, respectively. However, a common minimum plane can be determined. This problem can be avoided if the initial array has two different periods Λ in the x and the y directions, namely $\Lambda_x = s$ and $\Lambda_y = s/\cos\theta$.

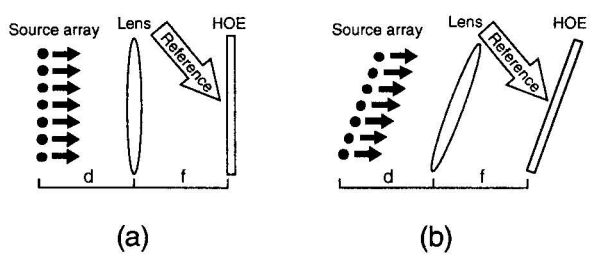

Fig. 7. Object waves (a) on-axis and (b) off-axis; the holographic optical element (HOE) becomes focusing for $d > f$ and nonfocusing for $d = f$.

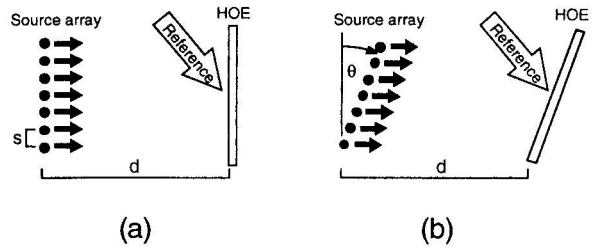

Fig. 8. Recording without a lens with spherical object waves by using the self-imaging properties of large periodic structures: (a) on axis, (b) off axis.

Because of the self-imaging properties, this method is suitable for large arrays only. Note that, depending on the position of the recording plane, this element becomes either a fan-out (overlapping) or a lenslet array (nonoverlapping beams).

Fan-out elements in volume holograms can be fabricated also by copying the phase structure of already existing fan-out elements as such, e.g., Dammann gratings. A simple image formation with a single lens would destroy the phase structure and therefore the properties of the fan-out. This can be avoided by using a 4-f imaging system, as shown in Fig. 9, which twice applies a Fourier transform, thereby conserving the phase distribution.[6] Analogous to Figs. 7 and 8, there also exists an off-axis arrangement of Fig. 9.

VIII. Conclusions

We have investigated the recording of efficient fan-out elements as volume holograms by using the coupled-wave theory. In contrast to the results published in the standard literature, we have found that the efficiency and uniformity of regular fan-out elements depend strongly on the relative phases of the object waves, if the thickness of the holographic emulsion is smaller than $t = \lambda/(n \tan\theta_0\Delta\alpha)$, where θ_0 is the angle of the reference wave and $\Delta\alpha$ the angle between the fan-out beams. A typical value is $t = 32$

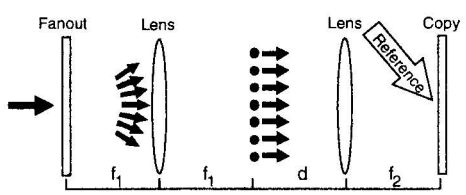

Fig. 9. 4-f system for copying fan-out elements, with magnification $m = f_2/f_1$, where $d = f_2$. Focusing power can be included if $d > f_2$.

μm for $\lambda = 488$ nm, $n = 1.5$, $\theta_0 = 30°$ and $\Delta\alpha = 1°$. High efficiency and uniformity can be achieved by optimized phases of the object beams, which minimize the intermodulations. At the same time the required dynamic range of the holographic material also becomes minimum.

The recording conditions are optimum if the irradiance of the object beam is uniform in the hologram plane. This can be achieved only in specific planes that are parallel to the object plane. As a consequence, only specific recording geometries are allowed. Several possible recording techniques for fabricating efficient and uniform fan-out elements have been presented.

IX. References

1. H. P. Herzig and R. Dändliker, "Holographic optical elements for use with semiconductor lasers," in *International Trends in Optics,* J. W. Goodman, ed., (Academic, New York, 1991), pp. 57–75.
2. H. Dammann and K. Görtler, "High-efficiency in-line multiple imaging by means of multiple phase holograms," Opt. Commun. **3,** 312–315 (1971).
3. S. J. Walker and J. Jahns, "Array generation with multilevel phase gratings," J. Opt. Soc. Am. A **7,** 1509–1513 (1990).
4. H. P. Herzig, D. Prongué, and R. Dändliker, "Design and fabrication of highly efficient fan-out elements," Jpn. J. Appl. Phys. **29,** L 1307–L 1309 (1990).
5. R. K. Kostuk, "Comparison of models for multiplexed holograms," Appl. Opt. **28,** 771–777 (1989).
6. B. Robertson, M. R. Taghizadeh, J. Turunen, and A. Vasara, "High-efficiency, wide-bandwidth optical fanout elements in dichromated gelatin," Opt. Lett. **15,** 694–696 (1990).
7. H. P. Herzig, P. Ehbets, D. Prongué, and R. Dändliker, "Fan-out elements by multiple beam recording in volume holograms," in *Holographic Optics III. Principles and Applications,* G. M. Morris, ed., Proc. Soc. Photo-Opt. Instrum. Eng. **1507,** 247–255 (1991).
8. I. Seyd-Darwish, P. Chavel, J. Taboury, and Y. Malet, "Array illuminator hologram based on the Talbot effect," in *Conference Record of the 1990 International Topical Meeting on Optical Computing* (Japan Society of Applied Physics, Tokyo, 1990), pp. 294–296.